Chapter 19
Volcanoes, Observations and Impact

Clifford Thurber and Stephanie Prejean

Glossary

Caldera	Large crater formed by collapse of an overlying structure when an eruption empties a magma reservoir.
Effusive	Eruption of fluid molten material that later solidifies.
Fumarole	A volcanic vent that emits hot gas.
Infrasound	Sound waves at frequencies below the range of human hearing (<20 Hz).
Interferogram	A pattern of satellite radar wave "fringes" formed by interference, analogous to the colorful pattern from light reflected by a thin film of oil or gas, that can indicate ground deformation.
Lahar	Heavy flow of mud, water, and debris triggered by interactions of hot material with ice of water or when heavy rain falls on recently erupted unconsolidated material.
Phreatic	Explosion caused by heating and expansion of ground water.
Pyroclastic	Composed of rock fragments ejected explosively from an erupting volcano.
Tremor	Continuous vibration of the ground related to magma movement.
Volatiles	Dissolved gases contained in magma.

C. Thurber (✉)
Department of Geoscience, University of Wisconsin-Madison, 1215 W. Dayton Street, 53706 Madison, WI, USA
e-mail: thurber@geology.wisc.edu

S. Prejean
Seismology, USGS Volcano Science Center, Alaska Volcano Observatory, 4200 University Drive, 99508 Anchorage, AK, USA
e-mail: sprejean@usgs.gov

Definition of the Subject

Volcanoes are critical geologic hazards that challenge our ability to make long-term forecasts of their eruptive behaviors. They also have direct and indirect impacts on human lives and society. As is the case with many geologic phenomena, the time scales over which volcanoes evolve greatly exceed that of a human lifetime. On the other hand, the time scale over which a volcano can move from inactivity to eruption can be rather short: months, weeks, days, and even hours. Thus, scientific study and monitoring of volcanoes is essential to mitigate risk. There are thousands of volcanoes on Earth, and it is impractical to study and implement ground-based monitoring at them all. Fortunately, there are other effective means for volcano monitoring, including increasing capabilities for satellite-based technologies.

In recent history, the destructive power of earthquakes and earthquake-induced tsunamis has been quite salient. Over the centuries and millennia, however, volcanic eruptions and eruption-induced tsunamis have had impacts that rival those of earthquakes, and in some cases have had a global reach. A prime example is the 1815 eruption of Tambora in Indonesia. That eruption is blamed for the catastrophic "Year without a Summer," when global cooling due to reflection of the Sun's energy by aerosols and ash injected into the atmosphere during the eruption led to massive crop failures and many deaths from starvation around the world [1, 2]. The Earth has also not witnessed a massive caldera-forming eruption, such as those that gave rise to Yellowstone and Long Valley calderas, since the formation of Toba caldera (also in Indonesia) about 75,000 years ago [3].

There is also a contrast between earthquakes and volcanoes in terms of predictability. Although reliable and effective earthquake prediction remains an elusive goal [4] and warning systems are operational in very few places (e.g., Japan), there are numerous examples of successful eruption forecasts and warnings. An example is the impressive success of the US Geological Survey's Volcano Disaster Assistance Program (VDAP), which reports dozens of successful eruption forecasts and warnings in the 25 years of the program's history [5]. Somewhat ironically, it is the monitoring of seismic activity that has been the key to VDAP's success.

Introduction

Although most of the world's magmatic activity occurs underneath the oceans, primarily along mid-ocean ridges, the discussion is restricted to volcanism on continents and islands. Within this subaerial class of volcanism, there are three main categories in terms of tectonic setting: subduction zones, hotspots, and continental rifts, with examples provided by Indonesia, Hawaii, and East Africa, respectively. Iceland is a special example of an above sea level section of mid-ocean ridge. The first-order classification of erupted products is based on silica content, with further distinctions based on alkali content (sodium and potassium)

[6] and the size of crystallized mineral grains. More silica-rich (felsic) lavas are predominant at subduction zones and more silica-poor (mafic) lavas are predominant at hotspots and continental rifts. In general, mafic lavas erupt more effusively whereas felsic lavas are more prone to explosiveness. For a thorough introduction to types of volcanoes and lavas and their potential for explosivity, the interested reader is referred to Lockwood and Hazlett [7].

The magnitude and violence of volcanic eruptions can be quantified in several ways. A common measure that is used in this entry is the Volcanic Explosivity Index (VEI) [8]. Volume of erupted material, ash cloud height, eruption duration, and qualitative observations describing eruption intensity are used in the calculation of VEI. Worldwide eruptions to date have been classified as VEI 0-8, with each increasing integer corresponding to an order of magnitude increase in eruption severity. The 1980 and 2004–2008 eruptions of Mount St. Helens, for example, are classified as VEI 4 (large eruption) and VEI 2 (moderate eruption), respectively. The largest eruptions of the twentieth century were of VEI 6, including the 1912 eruption of Novarupta on the Alaska Peninsula and the 1991 eruption of Mt. Pinatubo, Philippines. A second commonly used measure of eruption size is the dense-rock equivalent (DRE) of erupted material. This parameter specifies the actual amount of magma erupted and is dependent on careful field studies of erupted deposits. The Smithsonian Museum of Natural History keeps an updated database of these two eruption size parameters for recent and historical eruptions (http://www.volcano.si.edu/world/). Pyle [9] summarizes these and other measures of eruption sizes.

In this entry, the focus is mainly on geophysical observations of volcanoes and calderas as they pertain to eruption forecasting and prediction. Some key aspects of the impacts that eruptions have on humans and selected aspects related to sustainability have also been characterized.

Observations

The Role of Geologic Mapping

Our focus is primarily on geophysical volcano monitoring, but the importance of geologic mapping and associated studies cannot be overstated in providing the background information necessary to interpret these data correctly. In the case of erupting volcanoes, the past is generally the key to the present. Volcanoes often erupt similar magmas in similar volumes; thus, geological mapping to determine eruption histories provides a framework in which to interpret renewed unrest at a previously quiet volcano. In the case when a volcano's behavior diverges from its historical activity, knowledge of eruptive history allows us to understand how the magma system is evolving with time. Geologic mapping also characterizes the spatial distribution of hazards from previous eruptions including tephra fall, lahars

and pyroclastic and lava flows. These maps can have an important role in land use planning. In addition, careful petrologic, petrographic, and isotopic analyses of erupted material can provide valuable evidence regarding magma storage and transport history. These analyses complement the geophysical measurements described below to characterize the magmatic system at depth. For further details, the interested reader is referred to Decker [10], Simkin and Siebert [11], and Lockwood and Hazlett [7].

Seismology

Earthquake monitoring is certainly one of the most basic and widely used techniques for observing volcanic activity [12, 13]. In fact, seismic monitoring of volcanoes has generally been the most fruitful approach for short-term eruption prediction. The successes of the US Geological Survey's Volcano Disaster Assistance Program (VDAP) [5] in using simple measures of earthquake activity to predict eruptions is a remarkable testament to the value of real-time seismic monitoring for taking the pulse of a volcano in a state of unrest. VDAP has assisted with or directly provided more than 50 successful eruption forecasts and/or predictions for more than 30 volcanoes worldwide in the first 25 years of its history (1986–2011), using simple instrumentation and basic observations of seismicity and ground shaking [5].

Earthquakes associated with volcanoes are commonly grouped into four classes: volcano-tectonic (VT, predominant frequencies of 1–20 Hz), long-period (LP, predominant frequencies of 1–5 Hz), hybrid (VT event transitioning into an LP event), and very-long-period (VLP) [14, 15]. The former are generally believed to be normal brittle-failure earthquakes, although they commonly occur in swarms of similar-sized small events rather than a main shock-aftershock sequence style. This can be quantified by the log frequency versus magnitude (i.e., Gutenberg-Richter) relation (i.e., b-value), which is characterized by a linear trend with a slope around 1 for earthquakes on crustal faults but frequently has a higher slope, up to roughly two, for volcanic swarms.

The mechanism of LP's remains a subject of debate, centered mainly on the effect of fluids on the earthquake source versus the effects of wave propagation (path effects), and the connection between LP's and the phenomenon known as volcanic tremor is also controversial. Volcanic tremor is a more or less continuous signal lasting minutes to hours to days, with a comparable frequency content to LP's. Some researchers believe volcanic tremor is simply the superposition of repeated LP events or, in the case of harmonic tremor, VT events with the observed frequency content controlled by the earthquake repetition rate [16]. A somewhat more common hypothesis is that the tremor is due to resonant oscillations in a magma conduit or a nonlinear response to fluid flow through cracks [17, 18]. The initiation of volcanic tremor is clearly associated with the movement of magma and the potential for an eruption, and thus tremor is one of the important precursors

Fig. 19.1 Cartoon of the hypothetical relationship among VLP, LP, and HF (i.e., VT) earthquakes. In this model, the VLP source is upward flow of magma with volume change ΔV. Volatiles from the magma permeate the crust above the VLP event, triggering high frequency (HF) and LP earthquakes in a stress field with most and least compressive stress directions, σ_1 and σ_3 respectively, as shown (Modified from [39])
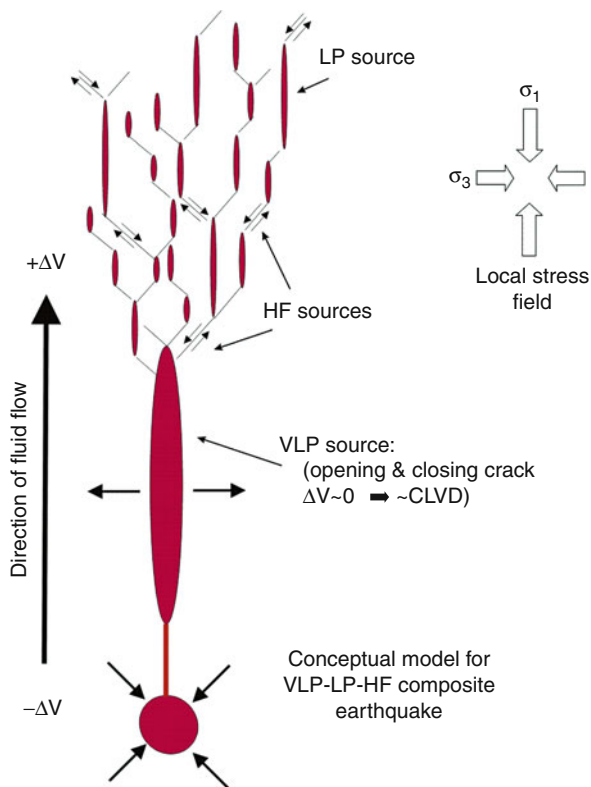
for eruption prediction [13]. In addition, deep LP's (typically 20–50 km depth) have been observed prior to a number of eruptions, presumably reflecting magma movement at depth [19–21], so additional focus has been placed on identifying these events. The nature of hybrid events is also debated, again centered on source versus path effects [22].

With the increasing use of broadband seismometers (instruments with a wide frequency range) in volcano monitoring, VLP earthquakes have been identified in many places [15, 23–38]. Similar to LP events, the source of VLP's is generally attributed to fluid-rock interaction, specifically transport of magma through the shallow crust. Waite et al. [38] for example, found that at Mount St. Helens, the VLP source is best modeled as a combination of volumetric and single-force components, the former due to compression and expansion of a shallow, magma-filled sill, and a smaller component of expansion and compression of a dike, and the latter due to mass transport in the magma conduit. A cartoon suggesting possible interrelationships among VLP, LP, and VT earthquakes based on the Hill fracture mesh concept [39] is shown in Fig. 19.1.

Some seismic path measurements have unveiled time dependencies that have been associated with eruptions, but for the most part these techniques have been applied retroactively. One of the earliest such studies was by Foulger et al. [40],

who found changes in the ratio of the velocity of P waves (primary, or compressional) to S waves (secondary, or shear) (i.e., Vp/Vs, equivalently Poisson's ratio) at Mammoth Mountain, California, that correlated spatially and temporally with increased tree kill due to CO_2 emission. They hypothesized that an increased presence of gas in fractures led to a reduction in Vp/Vs, which was imaged using seismic tomography. Such changes in Vp/Vs have also been identified at Mt. Etna, Italy [41]. Recently, temporal changes in seismic wave attenuation, in this case associated with magmatic activity, have been found at Mt. Ruapehu, New Zealand [42] as well as Mt. Etna [43].

Two other types of seismic path observations that have been reported to show temporal change associated with magmatic activity are shear wave splitting, which is caused by birefringence in the Earth, and ambient noise correlations, which yield an estimate of the wave propagation behavior (the Green's function) between two seismic stations. Miller and Savage [44] identified a change in the polarization direction of the fast shear wave at Mt. Ruapehu, which they associated with an eruption. Subsequent studies have also reported such changes elsewhere related to magmatic activity [45–49], but extreme care must be taken to separate spatial versus temporal variations. Brenguier et al. [50] compared a reference Green's function (created from 18 months of background or "ambient" noise data) to Green's functions from sequential 10-day periods of data at Piton de la Fournaise Volcano on La Reunion island and found shifts in apparent travel times corresponding to a small reduction in seismic velocity within the volcano. Their interpretation was that decreases in seismic velocity a few weeks before eruptions were related to preeruptive inflation of the volcanic edifice, presumably due to increased magma pressure.

Deformation

Uplift and subsidence associated with magmatic and eruptive activity have been recognized for centuries, with the Temple of Serapis in the town of Pozzuoli in Campi Flegrei caldera, Italy, being one of the most famous examples [51]. Geodetic surveying techniques, such as leveling and tilt measurements, began to be applied to volcanoes in the early twentieth century [52]. In the modern era, Global Positioning System (GPS) and interferometric synthetic aperture radar (InSAR), along with tilt, are the primary types of geodetic observations applied to the study and monitoring of volcanoes. The sensitivity of these different techniques is compared in Fig. 19.2. Continuous GPS (cGPS) and InSAR are quite complementary, with the former providing fine temporal resolution at particular points on the Earth's surface and the latter providing exceptional spatial resolution of position changes over a wide area for pairs of observation times. Deformation modeling is commonly done to estimate pressure changes in and the geometry of magma source zones.
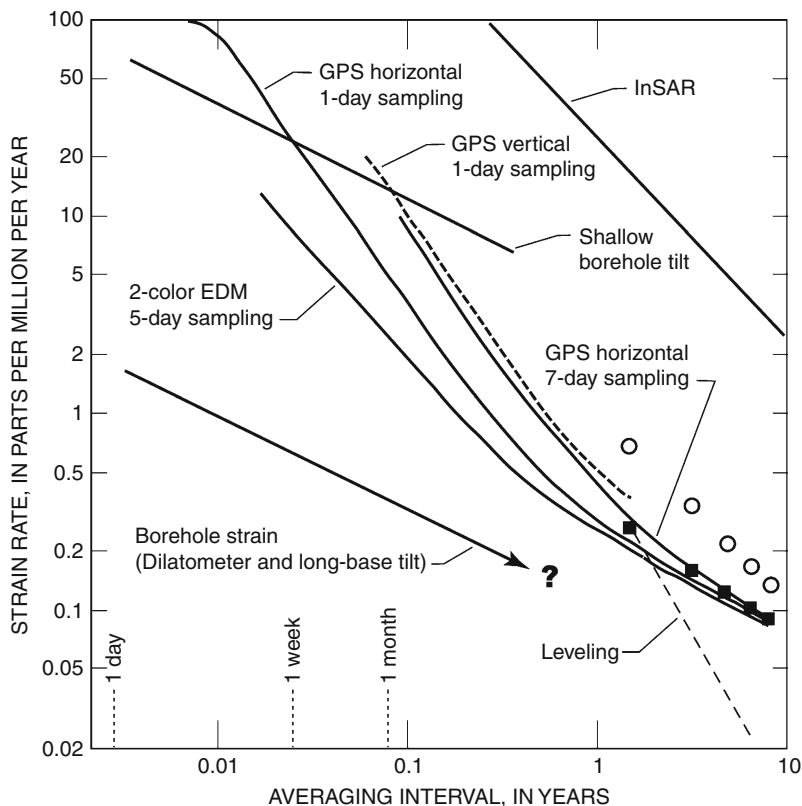
Fig. 19.2 Comparison of rate sensitivity for GPS, InSAR, borehole strainmeters at 200 m depth, and borehole tiltmeters (which measure the gradient in vertical deformation) at 2 m depth. The x-axis indicates the time period that may be spanned by the different data types. For example, daily GPS measurements may span 1 day or longer. The y-axis indicates the strain rate that can be resolved as a function of the period. Strain is the change in length (area or volume) per a unit length (area or volume), and thus is unitless and can be expressed as parts per million (ppm). As can be seen from the plot, the borehole tiltmeters and strainmeters are more sensitive than GPS at shorter periods, but at periods longer than a few days and a few months, respectively, GPS measurements provide better resolution of strain rates (Figure modified from [52])

GPS

Since the 1990s, GPS has become a central technique for volcano monitoring. Initial applications required repeated visits to benchmarks, known as campaign GPS. Continuous GPS (cGPS) has become relatively commonplace, allowing near-real-time tracking of site positions and, when multiple cGPS sites are available, a time history of volcano deformation. For example, with two cGPS sites on opposite sides of a volcano's summit or straddling a rift zone, relative changes in separation of the sites would reflect volcano inflation/deflation or rift zone extension/contraction. With enough sites, detailed modeling of deformation sources is

possible, providing constraints on the locations, depths, and pressure/volume changes of buried magma reservoirs and conduits. An example of the use of cGPS in monitoring an impending eruption at Augustine Volcano, Alaska [53] is described in some detail later.

GPS works by having a receiver on the surface of the Earth receive signals simultaneously from four or more satellites. These signals carry information about the signal origin time and the position of the satellite, so that determining the receiver position is done by trilateration, essentially analogous to locating an earthquake. The interested reader is referred to [52] for a lucid and comprehensive discussion of the details of this process.

GPS is not without its complications and limitations. GPS is a point measurement of position, so good spatial coverage requires multiple GPS sites. Data reduction requires knowledge of the GPS satellite orbits, which are known only approximately at any instant. Final orbital information is distributed by International GNSS Services (where GNSS stands for Global Navigation Satellite System) with about a 2-week delay [54]. The use of differential and kinematic GPS techniques effectively overcomes orbital (and some other) error effects, if only relative positions are desired. Atmospheric effects, due to ionosphere and troposphere delays, also impart positioning errors. Finally, elevation uncertainty is significantly greater than that for latitude and longitude.

InSAR

InSAR burst onto the geophysics scene in 1993 with the publication of the famous Landers, CA, earthquake interferogram on the cover of Nature [55]. Applications to volcanoes and calderas around the world followed soon thereafter, including Mt. Etna, Italy [56], Long Valley caldera, CA [57], Yellowstone caldera, WY [58], Piton de la Fournaise Volcano, La Reunion [59], a number of volcanoes in Alaska [60–65], the Galapagos Islands [66], Afar [67], Chile [68], and many more.

InSAR works by having a satellite (or constellation of satellites) acquire a pair of radar images of the same area on Earth from about the same point in space at different times, which are then combined, or interfered, to produce a map of the difference in phase of the two returned radar signals, represented by colored "fringes." The phase difference is related to the line-of-sight (LOS; i.e., in the direction of the satellite) displacement of the ground in the time between the two image acquisitions. Converting the phase differences into a map of LOS surface displacement is a process known as "unwrapping" [69, 70]. As in the case of GPS, source models can be derived to fit the observed displacements.

The spatial extent and resolution of InSAR coverage is extraordinary (scenes typically 10s to 100 km on a side with 1–30 m pixel size and <cm resolution of surface displacements). There are many more subtleties and complexities with InSAR data and their interpretation than for GPS, however. Repeated image acquisitions are limited by the configuration and orbits of the satellites. An accurate digital elevation model (DEM) is critical for removing the effects of topography

from the images. Noise in the data can lead to an incorrect assessment of LOS ground movement. Signal decorrelation, for example, due to vegetation variations, the presence of water, snow and ice, or steep topography, can yield areas with no usable signal. Atmospheric delay anomalies, due mainly to variations in tropospheric water content, can also cause artifacts in InSAR images. With the need for repeated imaging and the inherently limited temporal coverage for forming interferometric pairs, there is no guarantee that a good image can be created for a particular time interval of interest.

Tilt and Strain

Although far less ubiquitous in volcano monitoring settings than seismic and GPS instrumentation, tiltmeters and strainmeters are valuable observational tools that can provide complementary information about deformation. Both have remarkable sensitivity, with standard (bubble) tiltmeters able to measure the equivalent of 0.1 mm of uplift over a range of a kilometer (0.1 µrad, or 10^{-7} strain). Strainmeters can measure strain on the order of 10^{-11} to 10^{-12} (10 to 1 parts per billion). Tiltmeters have a number of advantages over strainmeters, including much lower cost, simpler installation, and, for biaxial sensors, the ability to provide information on the direction to the source of deformation. These advantages have been responsible for the much greater use of tiltmeters than strainmeters by volcano observatories. Due to their excellent sensitivity to vertical deformation, in contrast to GPS with its more precise determination of horizontal position, and real-time capability, tiltmeters can be of great value in volcanic crisis situations [52]. Strainmeters have also proven their value in long-term observatory settings, though, such as the successful prediction of an eruption of Hekla Volcano, Iceland, in 2000 [71].

Gravity

Gravity measurements can be used to infer vertical surface displacements with an accuracy comparable to GPS and some leveling techniques, but its real power comes from the ability to infer subsurface mass or density changes when surface deformation is constrained independently [52]. When uplift or subsidence occurs, the change in gravity can be compared to that predicted from the free-air gravity gradient. Deviations from the expected change in gravity reflect either an increase or decrease in mass in the subsurface [72], and the degree and sign of the difference constrains the density change. At Long Valley caldera, CA, for example, the combination of gravity and deformation observations allowed the inference of an intrusion of volatile-rich magma as the source of inflation in the period 1982–1999 [73].

For monitoring purposes, standard campaign-style gravity observations are of limited use, although such repeated measurements are vital for the types of research

noted above. There is significant monitoring potential with continuous networks of gravimeters [74]. An example is the continuous gravity network at Mt. Etna, Italy. Continuous gravity observations at the start of the 2002–2003 eruption, showing a reduced gravity decrease followed by recovery over a few hours, have been interpreted as indicating the initial opening of dry fractures that were subsequently filled by magma [75]. Although seismicity commenced several hours before the beginning of the gravity change, the detection of the opening of fractures would certainly be a key part of identifying the likely onset of an eruption.

Volcanic Gas

Detection of volcanic gas is an early indicator of magma ascent that can provide clues to speed of ascent, magma chemistry and explosivity, volume of intruding magma, and the state of the hydrothermal system at a volcano. As magma ascends in the Earth's crust, the decrease in confining pressure leads to exsolution of volatiles from the melt. Additional volatiles can also be released from the existing hydrothermal system as newly emplaced magma heats the surrounding rock. The resulting gases and fluids work their way toward the surface through fractures and can be observed through soil monitoring and space-, air-, and ground-based monitoring of fumaroles and gaseous plumes.

Interpreting the emission rates and compositions of volcanic gases to evaluate magmatic unrest is a challenging task. The compositions of volatiles released from magma vary with tectonic setting, melt composition, and pressure, but the most common gases include, in order of decreasing abundance, water, carbon dioxide (CO_2), sulfur dioxide (SO_2), and halogens. Arc volcanoes often host hydrothermal systems, crater lakes, or can be covered in snow and ice. For these reasons, volcanic gases emitted from arc volcanoes often have chemical reactions with water and other compounds on their way to the surface, which change their chemical form. For example, hydrolysis reactions can change SO_2 into H_2S and native sulfur [76]. This characteristic makes interpreting SO_2 emissions difficult at volcanoes with active hydrothermal systems (e.g., [77]). In contrast, because CO_2 exsolves from magma before other chemical species and because its chemical form is relatively stable as it ascends, its detection at the surface can be an early indicator that magma is ascending and accumulating beneath a volcano [78, 79]. The later appearance of increased SO_2 may then indicate continued magma ascent or drying out of the hydrothermal system. Given these complexities, it is necessary to consider the ratios of CO_2, SO_2, and H_2S to interpret the presence of these gases correctly. An additional complication in the interpretation of gas emissions is that most active volcanoes emit low levels of gas passively; therefore, background monitoring of quiescent time periods must be established before gas emissions associated with unrest can be interpreted correctly. Several strategies must be employed to measure the complete suite of emitted volcanic gases, including both continuous and

episodic ground and/or aircraft-based gas monitoring of fumaroles, satellite monitoring, and measurement of CO_2 flux through soils (see [80–82] for reviews of monitoring techniques).

Visual and Thermal Remote Sensing

Recent advances in satellite monitoring and ground-based and airborne remote sensing capabilities have revolutionized volcano monitoring and ash cloud tracking and provided a new perspective for understanding eruption dynamics. In the case of remote volcanoes that lack local seismic and GPS monitoring, satellite data often provide the only data stream documenting unrest and eruption. Data from satellites operated by the various international space agencies are primarily used for weather and climate research and forecasting, but are also used for volcano monitoring tasks including detecting and measuring anomalous thermal emissions, tracking ash clouds, and making visual observations. Rather than describe a complete list of satellite-based tools used in volcano studies, here the applicability of several satellite systems commonly used at US volcano observatories are highlighted, and readers are referred to more detailed reviews in the literature [82–84]. Some land- and aircraft-based imaging techniques are also briefly described.

When magma intrudes into a volcano, heat flow increases at the Earth's surface, resulting in hot fumaroles and fractures and melting of snow and ice. Thus, thermal remote sensing measurements can provide an early indicator of volcanic unrest in addition to defining the existence and spatial extent of lava flows, domes, and pyroclastic flows. The Moderate Resolution Imaging Spectroradiometer (MODIS) sensors on NASA research satellites and Geostationary Operational Environmental Satellite (GOES) and Advanced Very High Resolution Radiometer (AVHRR) sensors on NOAA satellites provide frequent, low resolution ($\sim$1 km pixel) data. Mid-infrared data (3.5–4 μm wavelength) from these sensors are used to study the extent and temporal development of lava and pyroclastic flows and to estimate effusion rates and thermal flux associated with an eruption.

Thermal infrared data from satellites (8–14 μm wavelength) are used to detect and track volcanic ash and gas clouds in the atmosphere, complementing ground- and satellite-based radar measurements of ash clouds. By comparing the brightness temperature difference in two different frequency bands, 11 and 12 μm, clouds containing ash can be discriminated from those containing only water using the Brightness Temperature Difference Method [85]. This method was used for tracking ash clouds from many eruptions (e.g., [86]) and has improved our understanding of the global atmospheric effects of large eruptions. The use of this technique to detect and measure volcanic ash clouds is limited by temporal coverage, atmospheric and cloud water content, tephra particle size, and thermal contrast between the cloud and the surface beneath it. Timing and intervals between images are dependent on satellite position and global location. For northern Pacific volcanoes,

for example, GOES data are available every 15 min, while AVHRR data are available 1–12 times per day depending on specific location [87]. Landsat TM and ETM+, Advanced Spaceborne Thermal Emission Reflection Radiometer (ASTER), and other high-resolution sensors provide a complementary dataset to these sensors. Although these data cannot be obtained in real time and images are less frequent, they provide high spatial resolution (15–90 m or better) for detailed visual and thermal observations. A recent compilation of capabilities to detect and measure volcanic clouds can be found in a European Space Agency report [88].

Thermal monitoring is not limited to satellite sensors. As an example of a sensor that can be hand held or mounted on an aircraft or tripod, the Forward Looking Infrared Radiometer (FLIR) camera is highlighted. FLIR surveys and installations often record simultaneous visual and infrared images or movies, providing maps of temperature distributions in ash clouds and on land surfaces. These images can be used to detect fumaroles, map pyroclastic flow deposits, and define spatial extent and structure of lava flows and domes. Frequently, gas emissions visually obscure volcanic activity, but FLIR thermal images can "see" through some gas, as demonstrated at volcanoes such as Mount St. Helens and Augustine [89, 90]. FLIR data have also been used successfully to characterize individual explosion characteristics at Stromboli Volcano [91].

Satellite remote sensing data are used for more than thermal imaging. Ultraviolet spectrometers, such as Total Ozone Mapping Spectrometers (TOMS) and the newer Ozone Monitoring Instrument (OMI) sensor operated by NOAA, can be used to map paths and concentrations of SO_2 clouds emitted from volcanoes by UV absorption of SO_2 in the atmosphere [92, 93]. Thanks to improved capabilities from the OMI sensor, scientists are better able to detect precursory SO_2 emissions in the atmosphere, to quantify eruptive SO_2 more accurately, and to track the SO_2 for longer periods of time. Thus, OMI data provide early indicators of magmatic unrest in addition to improving our understanding of eruption dynamics and hazard to aviation.

The remote sensing capabilities described here will undoubtedly evolve rapidly in the coming decade as technologies continue to advance and new satellites are launched. New remote monitoring tools will continue to emerge as well. For example, recent technical advances permit the measurement of volcanic lightning, both from ground and satellite sensors, to detect and study large ash clouds [94]. Improved resolution in digital cameras has permitted scientists to construct spectacular three-dimensional models of lava dome growth using aerophotogrammetric techniques [95].

Infrasound

Infrasound is the subaudible (<20 Hz) range of sound waves. Infrasound observations are made with either commercial or custom-built low-frequency microphones. These can be deployed individually or, more commonly, as arrays.

Array data can be stacked to diminish noise, which can be significant in these data, and can be used to determine the direction to the source. Infrasound disturbances can regularly be detected up to a few hundred kilometers from a volcano during eruptions. The use of infrasound for volcano monitoring was sufficiently rare at the beginning of the twenty-first century for the technique to be absent from some past reviews of volcano monitoring techniques (e.g., [12]), but now such observations are being made at dozens of volcanoes.

Infrasound observations are of great value for monitoring and quantifying eruptions, and are potentially useful for eruption prediction, especially in open-vent systems [96]. Unlike seismic observations, where variations in materials and structure in the Earth's crust along the seismic ray path have a strong influence on the recorded wavefield, the atmosphere alters infrasonic airwaves relatively little at high frequencies [97].This advantage makes infrasound quite useful for studying eruption dynamics and for quantitative comparisons of eruptions among different volcanoes [98]. Another advantage is that it is very difficult to distinguish between earthquakes at very shallow depths versus earthquakes directly associated with surface explosions using seismic data alone, but in many cases the absence or presence of an infrasound signal can serve to distinguish between the two possibilities and thus provide direct evidence that magmatically driven activity has reached the surface.

Infrasound data provide a new and unique perspective on the dynamics of volcanic eruption columns. Comparing ratios of seismic and acoustic energy between discrete explosions can offer compelling evidence for gas distributions in the magma column and eruption violence. Matoza et al. [99] have used infrasound data to investigate the spectra of volcanic jets and showed that they are similar to noise from aircraft jet engines. Infrasound has also been used to estimate the velocity of material ejected from volcanic vents during eruptions [100]. Observations of this sort could potentially be helpful in estimating ash output at erupting volcanoes when they cannot be observed directly.

Impacts

The literature on the impacts of volcanic eruptions is vast, so only brief and rather general information about selected topics is presented in this entry. The focus is on key primary and secondary volcanic hazards, and in particular those that have relatively immediate and direct impact. As a result, topics such as climatic effects are not covered here.

Lava Flows, Pyroclastics, and Tephra

Primary volcanic hazards that are direct eruption products can be categorized somewhat generally into lava flows, pyroclastic ejecta, and tephra. Lava is molten rock, and surface lava flows can travel many kilometers, or tens of kilometers in the case of basaltic tube-fed flows [101]. Their impact, though, will generally be spatially limited for any single eruption, although cases such as the decades-long rift eruption of Kīlauea Volcano are exceptions. Basaltic lava flows cause direct damage to the natural environment and human infrastructure, as well as igniting fires and/or touching off explosions that result in further damage. Fatalities due to basaltic lava flows are typically minimal, however, due to their modest flow rates, at least on terrain that is not particularly steep. Andesitic-dacitic stratovolcanoes, such as Mount St. Helens, grow blocky and viscous lava domes. Although generally limited in spatial extent to only the volcanic crater and its drainages, these domes can become unstable and fail, producing ash fall and hot block and ash flows down slope.

In contrast to lava flows, pyroclastic flows and surges (dense and dilute solid-gas mixtures, respectively, with a range of possible temperatures) travel at great speed, 10s of meters per second (m/s) to about 150 m/s (over 500 km/h), and large flows can travel 50 km or more from their source vents. The potential for destruction and death is summarily greater. For example, in the 1990s, deaths due to pyroclastic flows comprised the vast majority of directly caused mortality by volcanic eruptions [102].

Tephra is a general term encompassing various types of pyroclastic ejecta that are typically classified according to size, including blocks and bombs, lapilli, ash, and dust [7]. The larger fragments follow ballistic trajectories, whereas smaller particles can remain suspended in the atmosphere for some time (minutes to weeks) before falling to the surface. Tephra accumulations can amount to tens of centimeters to a few meters at distances of tens to hundreds of kilometers for very large eruptions [103]. Lockwood and Hazlett [7] point out that ballistic fragments are produced in greater abundance by smaller explosive eruptions. Annen and Wagner [102] report a similar number of deaths due to collapse of ash-covered roofs as due to pyroclastic flows and surges in the 1990s.

Lahars

Although a less familiar term to many, these mudflows or debris flows originating from volcanoes can have an enormous impact and cause many fatalities. Lahars can be generated directly and immediately by pyroclastic flows, or in a delayed manner upon collapse of volcanic deposits (for example, due to very heavy rainfall) or due to a lake breakout [104]. Flow rates are generally slower compared to pyroclastic flows, less than 10 m per second except on steep slopes.

A prime example of a lahar is from the eruption of Nevado del Ruiz, Colombia, in 1985. When the volcano erupted violently on the night of November 13, a massive lahar was initiated when pyroclastic flows caused massive melting of snow and glacial ice on the volcano. The lahar swept through and buried the town of Armero nearly 75 km away, resulting in more than 20,000 fatalities [105]. Sadly, the potential for a lahar from Nevado del Ruiz striking Armero had been well documented beforehand – mudflows from Nevado del Ruiz eruptions in 1595 and 1845 buried the same area [106]. Destructive lahars were also produced by the 1980 eruption of Mount St. Helens and the massive 1991 eruption of Mt. Pinatubo, Philippines.

Landslides, Lateral Blasts, and Tsunamis

Weaknesses in the interiors of volcanoes (fracturing and poorly consolidated material, hydrothermal alteration, etc.) leaves them prone to major landslides, which here is meant to encompass also avalanches and sector collapses. Avalanches are common on composite volcanoes, aka stratovolcanoes [7]. Some avalanches are triggered by the shaking from an earthquake. A landslide that grows and becomes more chaotic as it descends is termed a debris avalanche. At a larger scale, a sector collapse is the breaking away of a wedge-shaped flank of a volcano. When combined with an eruption, it can produce a lateral blast. Sector collapses are surprisingly common, at least on a geologic time scale. A number of Hawaii's volcanoes have experienced sector collapses, for example. The 1980 Mount St. Helens eruption began with a sector collapse producing a large debris avalanche, followed by a lateral blast and the initiation of a vertical eruption column. Lateral blasts are somewhat rare, but others have occurred at Arenal Volcano, Costa Rica [107] and Bezymianny Volcano, Russia [108]. For island volcanoes, there is the potential for landslides or especially sector collapses to produce a tsunami. The famous 1883 eruption of Krakatoa was accompanied by repeated tsunamis reportedly as high as 30–40 m around the Sunda Strait, killing tens of thousands of people [11]. Similarly, partial collapse of a volcano neighboring Unzen in 1792 generated a giant tsunami reaching heights of 60 m that caused on the order of 15,000 fatalities [7].

Volcanic Gases

As described above, volcanic gases are important indicators of magma transport, but they also represent a critical hazard. For example, although CO_2 is a significant component of the air we breathe regularly, this odorless, colorless gas is lethal at high concentrations. A tragedy involving CO_2 occurred in 1986 at Lake Nyos, Cameroon, a crater lake formed $\sim$400 years ago. Dissolved CO_2 accumulated in the lake and was released in a discrete event, killing all living things within a 25 km radius,

including 1,700 people [109]. In the United States, CO_2 emissions at Mammoth Mountain, CA, led to the deaths of four people between 1998 and 2006. CO_2 is far from the only harmful volcanic gas, however. For example, vog, a form of air pollution resulting from emissions of SO_2 and other volcanic gases, plagues the Island of Hawaii, as the actively erupting Kīlauea Volcano is a prolific producer of several gas species [110].

Eruption Forecasting: Strategies and Challenges

Earthquakes have been recognized to herald volcanic eruptions throughout history. For example, prior to the well-known eruption of Mount Usu, Japan in 1663, earthquake ground shaking caused local residents to evacuate. Eruption forecasting became a science with the advent of real-time seismic monitoring capabilities. Although earthquake observations still form the backbone of eruption forecasting, they are now complemented by more sophisticated analyses of seismic data and data from many other disciplines. Geodesy, gas chemistry analysis, satellite remote sensing, visual observations and high-resolution photography, petrography, and geochemistry all provide critically important indicators of the state of a magmatic system. Detectable manifestations of magma ascent vary widely between volcanoes based on several factors including the magma chemistry and crystallinity, the physical state of the volcano's conduit system and surrounding crust, the tectonic setting of the volcano, and time since last eruption. Thus, no one-size-fits-all forecasting approach exists. Modern volcano observatories are dynamic organizations that integrate a variety of data streams with knowledge of volcanic history to evaluate the state of unrest and potential future activity at a volcano.

In the United States volcano observatories use a color code alert level system to describe the state of volcano unrest [111]. One of the biggest challenges in forecasting volcanic eruptions and applying this alert system is assessing the time scale over which an eruption might occur. Here, the terms "forecast" and "prediction" as defined by [112] are used. Long-term forecasts, which address hazards on time scales of decades and centuries, are based on geological mapping of volcanoes and their deposits. Correct forecasts that describe likely hazards on time scales of hours to months based on geophysical and gas monitoring are common. However, reliable short-term predictions which specify the time and size of eruptions are difficult and fraught with complexities, not only in correctly interpreting the physical processes responsible for observations but in the delicacies of communicating with the emergency managers who coordinate societal response.

Almost all volcanic eruptions have earthquakes as precursors, but seismological response to magma ascent can vary significantly in character and in magnitude between volcanic systems. Although many eruptions of VEI 3 or smaller at frequently active volcanoes have only small earthquakes (magnitude (M) less than ~2.5) that may not be noticed without local seismic monitoring (e.g., [113]), large eruptions at volcanoes that erupt infrequently can have large earthquakes.

For example, the 1980 eruption of Mount St. Helens, the 1991 eruption of Pinatubo Volcano, and the 2008 eruption of Kasatochi Volcano all had associated earthquakes of M5.1 or greater [114]. The cataclysmic rhyolitic eruption of Novarupta in 1912, the largest eruption of the twentieth century, was associated with a staggering nine M6.0 and larger earthquakes [115].

Earthquakes at volcanoes often have unique characteristics that are not observed in purely tectonic systems, like the San Andreas Fault in California. The most obvious difference is that earthquakes at volcanoes tend to occur in swarms of many small earthquakes of similar size, as noted above. Unlike on tectonic faults, these earthquakes tend to increase in magnitude and frequency of occurrence with time before an eruption as magmatically driven pressure increases in the Earth's crust. The time history of seismicity is therefore critical in eruption forecasting. Earthquakes at volcanoes can also have distinctive frequency characteristics. LP and VLP earthquakes and volcanic tremor, for example, reflect fluid movement in the Earth's crust (see the "Seismology" section). Kasatochi Volcano, in the central Aleutian Islands, displayed the classic seismological eruption precursor sequence in 2008 [114]. In the 48 h prior to eruption, the rate and magnitude of earthquakes gradually increased, reflecting pressurization in the Earth's crust. In the 2 h prior to eruption and shortly after a M5.8 earthquake, strong volcanic tremor was observed, indicating that the earthquake likely increased permeability in the crust sufficiently for volatiles and magma to ascend rapidly.

Advanced analyses of seismic data, including some techniques described in the "Seismology" section, are actively being explored for eruption forecasting applications. For example, in some situations, real-time high-precision earthquake locations may be useful. In the 2000 eruption of Miyakejima, earthquakes were observed to migrate laterally as a dike was emplaced [116]. In other situations, however, such as the Long Valley caldera of California, earthquake locations can be misleading, as they reflect geothermally active areas and the fluid pathways rather than the location of magma itself.

The value of geodesy as an eruption forecasting tool was emphasized to the volcanological community during the 1980 eruption of Mount St. Helens. Prior to eruption, scientists at the Cascades Volcano Observatory documented a growing bulge on the north flank of the mountain. The eruption began as the bulge failed in an earthquake-induced landslide. The surprising and deadly horizontal blast of pyroclastic material that resulted highlighted the importance of deformation data in determining not only volume of magma intruded into volcanic edifices, but also eruption style and potential edifice collapse. Development of continuous GPS technologies in the late twentieth century made near-real-time deformation monitoring a reality. Later development of InSAR methods further improved the role of geodesy in volcano monitoring by providing spatially complete snapshots of volcano deformation. GPS is now a common component of volcano monitoring networks, although it is still significantly less common than seismic monitoring [117]. Dzurisin [118] describes monitoring strategies in which deformation data may be useful in making longer-term forecasts than are typically possible with seismic data alone.

Although seismic and geodetic monitoring are the most common data streams used in eruption forecasting, many other disciplines provide highly valuable information that can be critically important. For example, explosive eruptions of Bezymianny Volcano (Kamchatka), which generally begin with growth of a new lava dome that subsequently becomes unstable and fails, have been forecasted successfully based solely on thermal satellite data by KVERT (the Kamchatkan Volcanic Eruption Response Team). During the preeruptive stage of the 2009 eruption of Redoubt Volcano, Alaska, CO_2 levels provided one of the most conclusive early indicators that the unrest would advance to full eruption, rather than resulting in a stalled intrusion. Geochemical and physical tephra analyses often provide the first indicator that a juvenile magma is involved in an eruption, a critical indicator to understanding the size and potential explosivity of eruptions.

The challenge in interpreting geologic and geophysical indicators of eruption lies in determining the time scale and type of eruption, or even whether the magmatic activity will result in eruption at all. Earthquake swarms, for example, are common in volcanic and geothermal environments, and at least 2/3 and possibly as many as 9/10 of these do not result in eruption [119]. As magmas ascend, volatile exsolution and crystallization reduce overpressure and buoyancy in the magma body. Thus, most ascending magma bodies stall long before reaching the Earth's surface. Rejuvenation of a stalled magma body often involves an external trigger. Magma can be remobilized by many processes including accumulation of volatiles within the body, interaction of magma with water, a decrease in regional confining stress, or infusions of additional gas-rich magma from depth.

Eruption Forecasting: Case Studies

To demonstrate the variability in eruption precursors, two contrasting eruption case studies managed by the Alaska Volcano Observatory (AVO) are described: the 2006 eruption of Augustine Volcano and the 2008 eruption of Okmok Volcano. Both volcanoes were seismically and geodetically monitored, geologically mapped, and had documented historical eruptions. While the Augustine eruption exemplifies a successful eruption response, the Okmok eruption demonstrates how even thorough volcano monitoring does not guarantee that an eruption can be forecast.

The unrest preceding the 2006 eruption of Augustine Volcano, an andesitic stratovolcano located in the lower Cook Inlet of Alaska, proceeded in a "textbook" manner (see Power et al. [120] for a detailed review of the eruption). Scientists had observed this volcano erupt twice previously in 1976 and 1986, providing a template for interpreting unrest. Conveniently for the volcano observatory staff, the volcano closely followed the 1986 template. An increase in earthquake rate was first noted in late April 2005 (Fig. 19.3; [121]). Subsequently in fall 2005, airborne gas monitoring revealed that SO_2 output increased [122] and GPS monitoring showed that the volcano began to inflate [53]. These data together
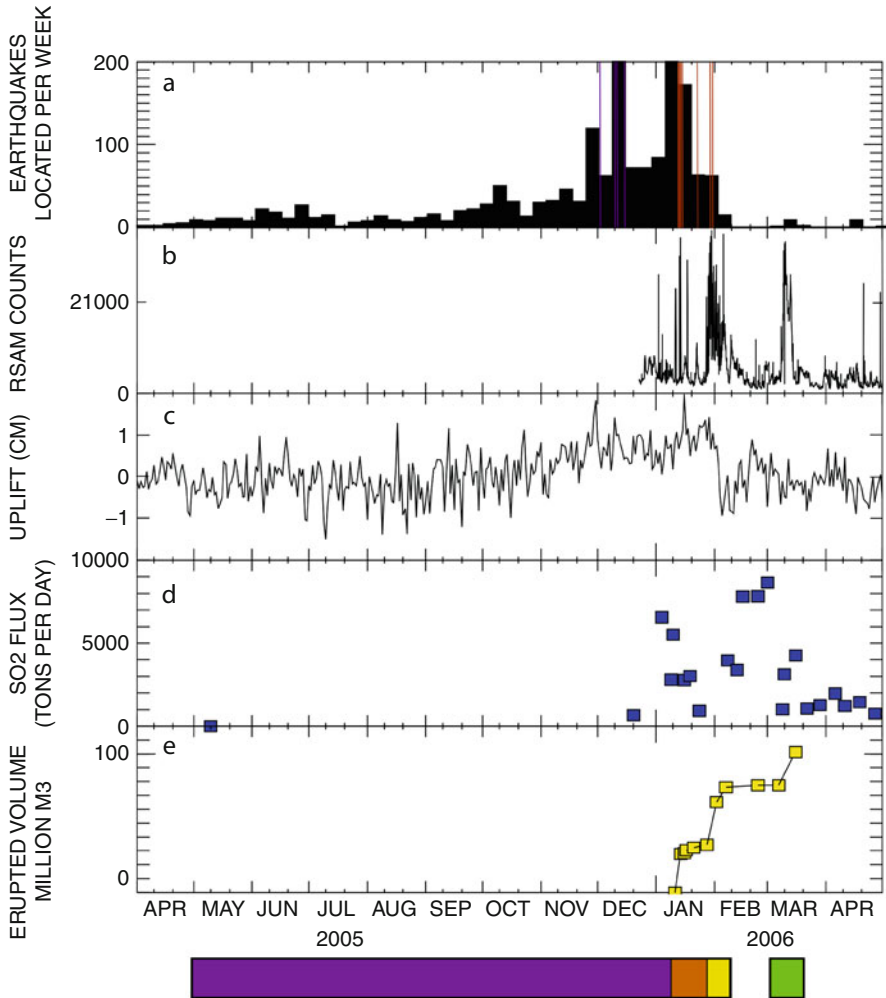
Fig. 19.3 Time history of the 2006 eruption of Augustine volcano, Alaska (From [121] and references therein). (**a**) Number of earthquakes located per week. *Purple* and *red lines* indicate phreatic and magmatic explosions, respectively; (**b**) hourly RSAM (reduced seismic amplitude measurement) from station AU13, indicating overall level of seismicity and tremor; (**c**) Uplift relative to GPS stations A59 and AV02; (**d**) SO_2 flux; and (**e**) erupted volume

strongly suggested that magma was ascending beneath and accumulating within the volcanic conduit. Thus, AVO raised the color code for level of concern from Green to Yellow in late November 2005 (see Neal et al. [123] for a detailed chronology of color codes). On December 2, 2005, the first small phreatic (steam) explosion occurred, presumably as ascending magma interacted with water in the conduit. In response to this event, the color code was raised to Orange. Explosions of this type are often interpreted as "vent clearing" events, as they open the pathway for

new magma to ascend. In the following month, anomalous activity waxed and waned, but continued to increase gradually in severity, until January 11, 2006, when the volcano had its first significant ash-rich explosion of magma, and the color code was raised to Red. This phase of the eruption continued with intermittent explosions for 2 weeks. Subsequently, the volcano effused small amounts of ash nearly continuously for two additional weeks, through early February 2006. The eruption gradually transitioned to effusive lava dome growth as magma was degassed sufficiently to permit more passive eruption of andesitic magma. A lava dome grew at the volcano's summit through mid-March 2006 and the volcano subsequently returned to a quiet state. This series of increased unrest, phreatic explosions, magmatic explosions, and effusion is relatively common in andesitic stratovolcanoes and relatively easy to forecast correctly.

Okmok Volcano, a large caldera located in the eastern Aleutian Islands, had a history of small explosions and basaltic and basaltic-andesite lava flows prior to the 2008 eruption, with the most recent of these in 1997. In the decade between eruptions, earthquakes were rare and volcanic tremor was common enough to be considered background activity for the volcano. GPS and InSAR data revealed that Okmok experienced periods of both inflation and deflation since at least 2000 and was inflating continuously for 6 months prior to eruption [124, 125]. On the morning of July 12, 2008, the volcano was quiet and deformation data revealed no unusual increase in the rate of inflation. However by 11:30 AM AKDT of that day, seismicity ramped up dramatically from quiescence to near constant small earthquakes of $M < 3$ (Fig. 19.4) over a 60 min interval. Phreato-magmatic eruptive activity followed the first earthquake in the series by less than 2 h. In response, AVO raised the color code from Green directly to Red. Unlike previous effusive lava flow eruptions at Okmok Volcano, the 2008 eruption propelled ash into the atmosphere, affecting north Pacific air traffic for several months. Geologic studies of the eruption deposits reveal that the interaction of magma with a large quantity of groundwater likely drove the eruption to be more explosive and ash-rich than previous eruptions at the volcano [126]. Johnson et al. [127] speculate that prior to the eruption, the shallow open magmatic system was able to degas easily, preventing build up of overpressure and earthquakes. Either a subtle addition of melt or sudden contact with water may have triggered the eruption. This scenario is a worst-case example in terms of forecasting. It is arguably the only eruption at a monitored United States volcano with a well-established seismic network that was not forecast since 1989.

Volcano-Earthquake Interactions

Volcanism and large earthquakes near plate margins are two different manifestations of plate tectonics; thus, over time scales of millennia the processes are closely linked. How earthquakes and volcanoes affect one another over shorter
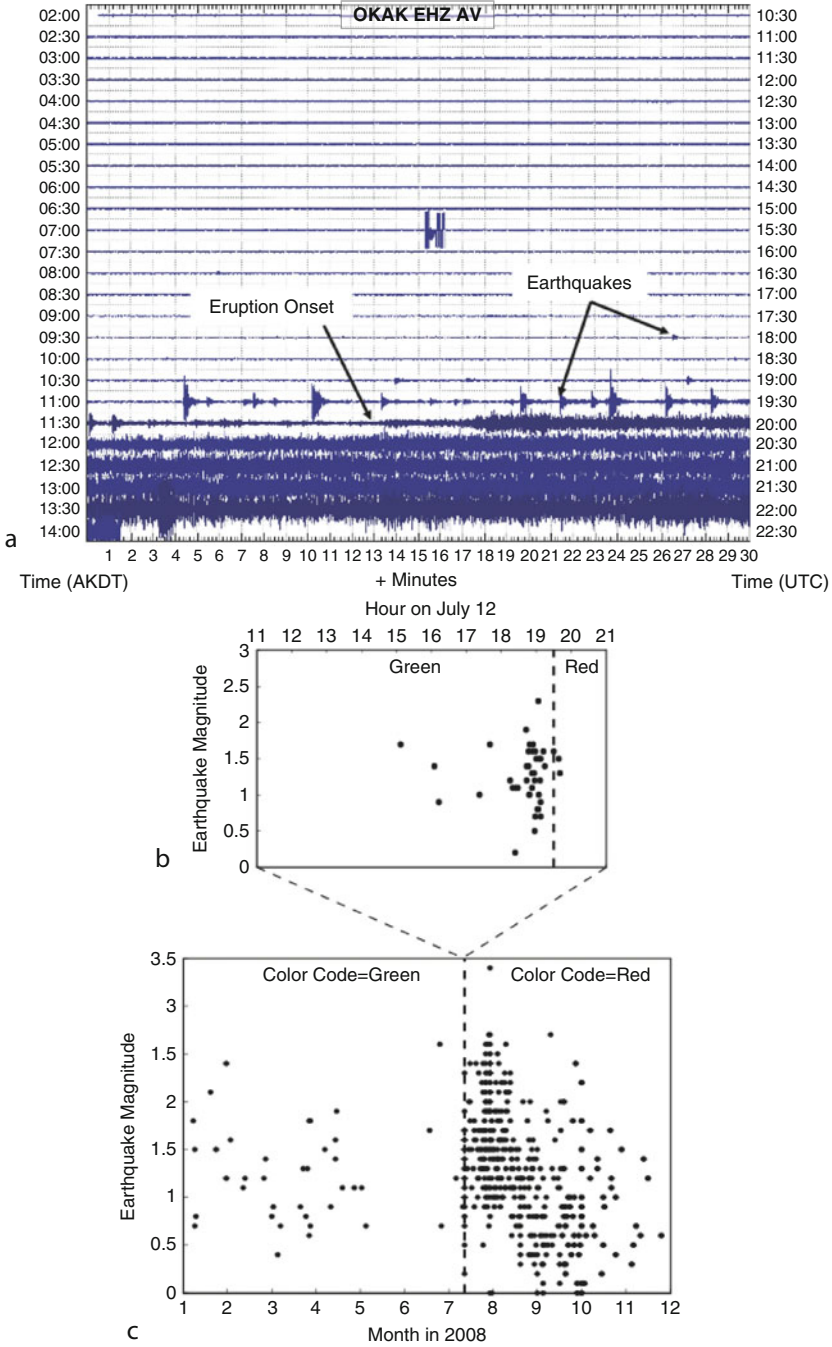
Fig. 19.4 Seismicity related to the 2008 eruption at Okmok caldera, Alaska, from [125]. (**a**) Twelve hours helicorder plot of seismic data from station OKAK, showing quiescence in the hours prior to eruption. (**b**) Located earthquakes over 10 h near the time of eruption onset. (**c**) Located earthquakes at Okmok by the Alaska Volcano Observatory in 2008. *Colors* indicate color code alert level assigned by the Alaska Volcano Observatory

timescales, such as days to months, remains an open and intriguing problem. One frequently asked question in times of crisis is, "can a large earthquake trigger eruption of a nearby volcano?" There are a few compelling examples of eruptions following large earthquakes that suggest a causal relationship between the two, such as the brief eruption of Kīlauea Volcano following the M 7.2 Kalapana Hawaii earthquake in 1975 and the eruption of Puyehue-Cordon Caulle Volcano immediately following the M 9.5 Chile earthquake in 1960. However, it is also true that large earthquakes occur commonly without related eruptions. For example, although the 1964 M9.2 Alaska earthquake occurred in a region with dozens of active volcanoes, the only report of volcanic activity in the subsequent months was a suggestion of increased steaming at Wrangell Volcano, Alaska. Establishing a causal, statistically significant relationship between a large earthquake and a subsequent volcanic eruption is difficult, as it requires an accurate understanding of the probabilities of each event occurring independently. This in turn requires a robust long-term record of eruption and earthquake occurrence, which is rarely available. Studies to date [128–130] suggest that evidence exists for earthquake-triggered eruptions, but it is not a common phenomenon. In the rare occasion where this does occur, there are several possible mechanisms that may explain eruption triggering [131]. Static stress changes in the Earth's crust related to the earthquake may change the confining pressure on a magma reservoir, destabilizing it. Alternatively, high frequency dynamic seismic waves may destabilize the magma by causing bubble nucleation or increasing convection within the reservoir. Finally, violent shaking may cause fractures, landslides, or other changes to the crustal volume surrounding a shallow magma reservoir, leading to eruption.

Large earthquakes commonly affect volcanoes in subtle ways, however. Following the 1992 M 7.3 Landers, California earthquake, volcanic and geothermal areas across the western United States showed an increase in earthquake activity [132]. Since that time, small earthquakes triggered at great distances by surprisingly small amplitude oscillatory seismic waves from large earthquakes (≤ 0.01 MPa dynamic stress change) have been documented at many areas around the world (see Prejean and Hill [133] for review). Although dynamic triggering of small earthquakes happens in many environments, volcanoes appear to be particularly susceptible to dynamic earthquake triggering [133]. A range of physical models have been proposed to explain how small amplitude dynamic waves trigger earthquakes, including changing fluid pathways in delicate hydrothermal systems, changing the crustal stress field by disrupting magma chambers, and directly exceeding the frictional strength of faults [134]. Most models require very high pore-fluid pressures in the volume where the triggered earthquakes occur.

Volcanoes and Sustainability

The focus of this section is on three direct and immediate connections between volcanoes and sustainability. One is the societal hazard factor – as with other

geologic hazards, population growth puts more and more people at risk for possible volcanic impacts. A second, related impact is eruption effects on aviation, which received global attention in 2010 due to the eruption of Eyjafjallajökull Volcano in Iceland. The third is magmatic activity as a source of geothermal energy. Areas being tapped for commercial-scale geothermal energy are in regions of magmatic activity if not actually on the flanks of a volcano (e.g., the Puna Geothermal Venture on Kilauea). Longer-term connections between volcanoes and sustainability, including climatic effects and connections to ore deposits, are not covered here but are discussed in numerous sources (e.g., [135, 136]).

Volcanoes and Human Population

About 10% of the world's population lives on or near active volcanoes [137], and this percentage is steadily increasing with time. Lockwood and Hazlett [7] estimate that more than 100 million people live in areas near calderas that have been subjected to pyroclastic flows. There have been a number of large eruptions in the past several centuries, but nothing rivaling the very large explosive volcanic eruptions ("super volcanoes") that are present in the geologic record [138], so in historic times, humans have not experienced the full impact that volcanic eruptions can produce. However, the number of eruptions causing fatalities has steadily increased each century since the 1500s, which Simkin et al. [139] attribute to increased global population, as opposed to an increase in the frequency of eruptions.

Quantifying the hazard from volcanic eruptions is certainly a challenge, especially considering the shortness of the historic record in comparison to the frequency of occurrence of large to very large eruptions (centuries to many millennia). Interestingly, eruption size on the VEI scale [8] follows a roughly linear size-log frequency distribution, similar to the Gutenberg-Richter relation for earthquakes. Simkin and Siebert [11] found that VEI 6 eruptions occur about once or twice a century, VEI 5 about once per decade, VEI 4 once or twice a year, etc. Ewert and Harpel [140] combined the global distributions of population and volcanoes to derive a Volcano Population Index (VPI), and applied it to Central America. VPI quantifies the population within 5 (VPI5) or 10 (VPI10) km of a volcanic system, corresponding to eruptions of VEI 2–4. They found that roughly 2.5 million people were at risk as measured by VPI10, and also suggested that only Indonesia might have a larger exposed population than Central America. As in the case of earthquake and tsunami hazards, population centers in harm's way of a possible future eruption are certainly not going to relocate. Mitigation, warning strategies and systems, and education efforts are therefore essential.

Volcanoes and Aircraft

The prolonged eruption of Eyjafjallajökull in Iceland in 2010 is a prime example of the impact volcanic eruptions can have on air travel. That disruption cost airlines billions of dollars [141], and certainly caused additional losses to businesses and people impacted by the shut down in air travel. The most critical hazard is the intake of ash into jet engines, which can severely damage engine parts and potentially cause engine failure. For example, KLM Flight 867, with 245 passengers and crew on board, encountered the ash cloud from the eruption of Alaska's Redoubt Volcano on December 15, 1989, causing all four engines to shutdown. The airplane plunged nearly 15,000 ft before the pilots were able to restart the engines and ultimately land safely, albeit with tens of millions of dollars of damage to the airplane. In the 1980s through the mid 1990s, about one airplane per year experienced damage from volcanic ash on North Pacific air routes [142]. The USGS, along with Alaskan state agencies, established the Alaska Volcano Observatory in 1988 in large part to address the volcanic ash-aircraft problem in that region.

Assessing and monitoring the ash hazard to aircraft requires the application of essentially all the tools available. This includes forecasting, monitoring, and prediction efforts prior to an eruption and 24/7 geophysical monitoring and remote sensing to track eruptive activity and the spread of ash clouds during an eruption. Because volcanic ash from large eruptions can remain in the atmosphere at flight altitudes for weeks or longer, circling the globe multiple times, addressing the hazard requires international cooperation of air traffic controllers, scientists, and weather agencies. As air passenger and cargo air traffic continues to increase globally, the risk will escalate.

Volcanoes and Geothermal Energy

Volcanoes can provide part of the solution to global energy needs, as heat generated inside the Earth can be harnessed for geothermal energy. Although volcanic activity is not required for geothermal energy production in enhanced geothermal systems (EGS), such as that at Soultz-sous-Forets, France, volcanic activity brings heat nearer the Earth's surface, potentially lowering the cost of energy production. The United States is currently the largest producer of geothermal energy [143], although many other countries are developing their own resources. Successful geothermal energy plants located on active volcanoes or above magma chambers are currently in operation in the United States at Kīlauea Volcano in Hawaii, the Long Valley caldera, California, and many other sites in California, Nevada, and Idaho, although in total geothermal sources provided less than a half a percent of the electricity in the US in 2009 [144]. The potential to produce geothermal energy at additional volcanoes in Alaska and the Pacific Northwest is being explored aggressively. Most current geothermal energy operations involve tapping hot ground water. In contrast,

the Geysers, California – the largest geothermal field in the United States – is a dry steam field that taps superheated steam.

A potential risk associated with geothermal power is triggering earthquakes. Generally, earthquakes associated with geothermal production are small (M < 2), but occasional larger earthquakes have disrupted communities, most notably in Basel, Switzerland. A second less common but significant risk to geothermal energy production at active volcanoes in Hawaii and Alaska involves eruptions disrupting the energy supplies and potentially destroying infrastructure.

Future Directions

Technological developments to improve and expand observational capabilities are likely to have the greatest impact on the development of volcano studies in the future [145]. An example is the use of autonomous sensor networks [146, 147]. The combination of ease of deployment and networked communication makes such systems extremely appealing for volcano monitoring. Deployment of a constellation of radar satellites with wavelengths that are tuned to "see" through vegetative cover could cut InSAR repeat observation cycles to intervals of days, allowing for high spatial resolution observations of deformation on a time scale of use for eruption forecasting. One can imagine a day when radar satellites detect significant deformation of a volcano anywhere in the world (on land), an autonomous sensor network is deployed rapidly (e.g., [148]), and a team of volcanologists forecasts the activity as the episode of unrest unfolds, comparable to severe storm forecasting.

In closing, the concern that population growth and expanding commercialism (especially air travel) will inexorably lead to increasing impact of volcanic activity on humans, either directly or indirectly, is reiterated. Although volcanoes certainly cannot be controlled, monitoring technologies and strategies for forecasting and predicting their behavior can be effective. It therefore seems clear that increased efforts in volcano monitoring are required to mitigate future risks.

Bibliography

1. Oppenheimer C (2003) Climatic, environmental and human consequences of the largest known historic eruption: Tambora volcano (Indonesia) 1815. Prog Phys Geogr 27:230–259
2. Stothers RB (1984) The great Tambora eruption in 1815 and its aftermath. Science 224:1191–1198
3. Rose WI, Chesner CA (1987) Dispersal of ash in the great Toba eruption, 75 ka. Geology 15:13–917
4. Hough S (2009) Predicting the unpredictable: the tumultuous science of earthquake prediction. Princeton University Press, Princeton
5. White RA, McCausland WA, Lockhart AB (2011) Volcano monitoring: keep it simple – less can be more during volcano crises; 25 years of VDAP experience. Seism Res Lett 82:330

6. Le Bas MJ, Le Maitre RW, Streckeisen A, Zanettin B (1986) A chemical classification of volcanic rocks based on the total alkali-silica diagram. J Petrol 27:745–750
7. Lockwood JP, Hazlett W (2010) Volcanoes – global perspectives. Wiley-Blackwell, Hoboken
8. Newhall CG, Self S (1982) The volcanic explosivity index (VEI): an estimate of explosive magnitude for historical volcanism. J Geophys Res 87:1231–1238
9. Pyle DM (2000) Sizes of volcanic eruptions. In: Sigurdsson H, Houghton BF, McNutt SR, Rymer H (eds) Encyclopedia of volcanoes. Academic Press, San Diego
10. Decker RW (1986) Forecasting volcanic eruptions. Ann Rev Earth Planet Sci 14:267–291
11. Simkin T, Siebert L (1994) Volcanoes of the world. Geoscience, Tucson
12. McNutt SR (1996) Seismic monitoring of volcanoes: a review of the state-of-the-art and recent trends. In: Scarpa R, Tilling R (eds) Monitoring and mitigation of volcano hazards. Springer, Berlin
13. McNutt SR (2000) Seismic monitoring. In: Sigurdsson H, Houghton BF, McNutt SR, Rymer H (eds) Encyclopedia of volcanoes. Academic Press, San Diego
14. Lahr JC, Chouet BA, Stephens CD, Power JA, Page RA (1994) Earthquake classification, location, and error analysis in a volcanic environment: implications for the magmatic system of the 1989–1990 eruptions at Redoubt volcano, Alaska. J Volcanol Geotherm Res 62:137–151
15. Hill DP, Dawson P, Johnston MJS, Pitt AM, Biasi G, Smith K (2002) Very-long-period volcanic earthquakes beneath Mammoth Mountain, California. Geophys Res Lett 29:1370. doi:10.1029/2002GL014833
16. Hotovec AJ, Prejean SG, Vidale JE, Gomberg J (in press) Strongly gliding harmonic tremor during the 2009 eruption of Redoubt volcano. J Volcanol Geotherm Res
17. Chouet B (1985) Excitation of a buried magmatic pipe: a seismic source model for volcanic tremor. J Geophys Res 90:1881–1893
18. Julian B (1994) Volcanic tremor: nonlinear excitation by fluid flow. J Geophys Res 99:11859–11877
19. White RA (1996) Precursory deep long-period earthquakes at Mount Pinatubo: spatial-temporal link to a basaltic trigger. In: Newhall CG, Punongbayan RS (eds) Fire and mud: eruptions and lahars of Mount Pinatubo, Philippines. University of Washington Press, Seattle
20. Power JA, Stihler SD, White RA, Moran SC (2004) Observations of deep long-period (DLP) seismic events beneath Aleutian arc volcanoes; 1989–2002. J Volcanol Geotherm Res 138:243–26
21. Mavonga T, Zana N, Durrheim RJ (2010) Studies of crustal structure, seismic precursors to volcanic eruptions and earthquake hazard in the eastern provinces of the Democratic Republic of Congo. J Afr Earth Sci 58:623–633. doi:10.1016/j.jafrearsci.2010.08.008, ISSN 1464-343X
22. Harrington RM, Brodsky EE (2007) Volcanic hybrid earthquakes that are brittle-failure events. Geophys Res Lett 34:L06308. doi:10.1029/2006GL028714
23. Kawakatsu H, Ohminato T, Ito H, Kuwahara Y (1992) Broadband seismic observation at the Sakurajima volcano, Japan. Geophys Res Lett 19:1959–1962
24. Kawakatsu H, Ohminato T, Ito H (1994) 10s-period volcanic tremors observed over a wide area in southwestern Japan. Geophys Res Lett 21:1963–1966. doi:10.1029/94GL01683
25. Neuberg J, Luckett R, Ripepe M, Braun T (1994) Highlights from a seismic broadband array on Stromboli volcano. Geophys Res Lett 21:749–752. doi:10.1029/94GL00377
26. Kaneshima S, Kawakatsu H, Matsubayashi H, Sudo Y, Tsutsui T, Ohminato T, Ito H, Uhira K, Yamasato H, Oikawa J, Takeo M, Iidaka T (1996) Mechanism of phreatic eruptions at Aso volcano inferred from near-field broadband seismic observations. Science 273:642–645
27. Ohminato T, Chouet BA, Dawson P, Kedar S (1998) Waveform inversion of very long period impulsive signals associated with magmatic injection beneath Kilauea volcano. J Geophys Res 103:23839–23862. doi:10.1029/98JB01122

28. Arciniega-Ceballos A, Chouet BA, Dawson P (1999) Very long period signals associated with vulcanian explosions at Popocate´petl volcano, Mexico. Geophys Res Lett 26:3013–3016. doi:10.1029/1999GL005390

29. Legrand D, Kaneshima S, Kawakatsu H (2000) Moment tensor analysis of near-field broadband waveforms observed at Aso volcano, Japan. J Volcanol Geotherm Res 101:155–169. doi:10.1016/S0377-0273(00)00167-0

30. Nishimura T, Kobayashi T, Ohtake M, Sato H, Nakamichi H, Tanaka S, Sato M, Ueki S, Hamaguchi H (2000) Source process of very long period seismic events associated with the 1998 activity of Iwate volcano, northeastern Japan. J Geophys Res 105:19135–19147. doi:10.1029/2000JB900155

31. Rowe CA, Aster RC, Kyle PR, Dibble RR, Schlue JW (2000) Seismic and acoustic observations at Mount Erebus volcano, Ross Island, Antarctica, 1994–1998. J Volcanol Geotherm Res 101:105–128. doi:10.1016/S0377-0273(00)00170-0

32. Kumagai H, Ohminato T, Nakano M, Ooi M, Kubo A, Inoue H, Oikawa J (2001) Very-long-period seismic signals and caldera formation at Miyake Island, Japan. Science 293:687–690. doi:10.1126/science.1062136

33. Almendros J, Chouet B, Dawson PB, Bond T (2002) Identifying elements of the plumbing system beneath Kilauea volcano, Hawaii, from the source locations of very-long-period signals. Geophys J Int 148:303–312

34. Hidayat D, Voight B, Chouet B, Dawson P, Ratdomopurbo A (2002) Source mechanism of very-long-period signals accompanying dome growth activity at Merapi volcano, Indonesia. Geophys Res Lett 29. doi:10.1029/2002GL015013

35. Aster R, Mah S, Kyle P, McIntosh W, Dunbar N, Johnson J, Ruiz M, McNamara S (2003) Very long period oscillations of Mount Erebus volcano. J Geophys Res 108:2522. doi:10.1029/2002JB002101

36. Chouet B, Dawson P, Ohminato T, Martini M, Saccorotti G, Giudicepietro F, Luca GD, Milana G, Scarpa R (2003) Source mechanisms of explosions at Stromboli volcano, Italy, determined from moment-tensor inversions of very-long-period data. J Geophys Res 108:2019. doi:10.1029/2002JB001919

37. Chouet B, Dawson P, Arciniega-Ceballos A (2005) Source mechanism of Vulcanian degassing at Popocate´petl volcano, Mexico, determined from waveform inversions of very long period signals. J Geophys Res 110:B07301. doi:10.1029/2004JB003524

38. Waite GP, Chouet BA, Dawson PB (2008) Eruption dynamics at Mount St. Helens imaged from broadband seismic waveforms: interaction of the shallow magmatic and hydrothermal systems. J Geophys Res 113:B02305. doi:10.1029/2007JB005259

39. Hill DP (1977) A model for earthquake swarms. J Geophys Res 82:1347–1352. doi:10.1029/JB082i008p01347

40. Foulger GR, Julian BR, Pitt AM, Hill DP, Malin P, Shalev E (2003) Three-dimensional crustal structure of Long Valley Caldera, California, and evidence for the migration of CO_2 under Mammoth Mountain. J Geophys Res 108:B3. doi:10.1029/2000JB000041

41. Patanè D, Barberi G, Cocina O, De Gori P, Chiarabba C (2006) Time resolved seismic tomography detects magma intrusions at Mount Etna. Science 313:821–823

42. Titzschkau T, Savage M, Hurst T (2010) Changes in attenuation related to eruptions of Mt. Ruapehu volcano, New Zealand. J Volcanol Geotherm Res 190:168–178

43. De Gori P, Chiarabba C, Giampiccolo E, Martinez-Arevalo C, Patane D (2011) Body wave attenuation heralds incoming eruptions at Mount Etna. Geology 39:503–506

44. Miller V, Savage M (2001) Changes in seismic anisotropy after volcanic eruptions: evidence from Mount Ruapehu. Science 293:2231–2233

45. Patanè D, De Gori P, Chiarabba C, Bonaccorso A (2003) Magma ascent and the pressurization of Mount Etna's volcanic system. Science 299:2061–2063

46. Volti T, Crampin S (2003) A four-year study of shear-wave splitting in Iceland: 2. Temporal changes before earthquakes and volcanic eruptions. In: Nieuwland DA (ed) New insights into

structural interpretation and modeling, Geological Society of London, Special Publication 212. Geological Society, London, pp 135–149

47. Musumeci C, Cocina O, De Gori P, Patanè D (2004) Seismological evidence of stress induced by dike injection during the 2001 Mt Etna eruption. Geophys Res Lett 31:L07617. doi:10.1029/2003GL019367

48. Bianco F, Scarfı L, Del Pezzo E, Patanè D (2006) Shear wave splitting changes associated with the 2001 volcanic eruption on Mt. Etna. Geophys J Int 167:959–967

49. Roman DC, Savage MK, Arnold R, Latchman JL, De Angelis S (2011) Analysis and forward modeling of seismic anisotropy during the ongoing eruption of the Soufrière Hills volcano, Montserrat, 1996–2007. J Geophys Res 116:B03201. doi:10.1029/2010JB007667

50. Brenguier F, Shapiro N, Campillo M, Ferrazzini V, Duputel Z, Coutant O, Nercessian A (2008) Towards forecasting volcanic eruptions using seismic noise. Nat Geosci 1:126–130

51. Poland M, Hamburger M, Newman A (2006) The changing shapes of active volcanoes: history, evolution, and future challenges for Volcano Geodesy. J Volcanol Geotherm Res 150:1–13

52. Dzurisin D (2007) Volcano deformation: geodetic monitoring techniques. Springer, Berlin

53. Cervelli PF, Fournier TJ, Freymueller JT, Power JA, Lisowski M, Pauk BA (2010) Geodetic constraints on magma movement and withdrawal during the 2006 eruption of Augustine volcano. In: Power JA, Coombs ML, Freymueller JT (eds) The 2006 eruption of Augustine volcano, Alaska, U.S. Geological Survey Professional Paper 1769. U.S. Geological Survey, Reston, pp 427–452

54. Dow JM, Neilan RE, Rizos C (2009) The International GNSS service in a changing landscape of Global Navigation Satellite Systems. J Geodesy 83:191–198. doi:10.1007/s00190-008-0300-3

55. Massonnet D, Rossi M, Carmona C, Adragna F, Peltzer G, Feigl K, Rabaute T (1993) The displacement field of the Landers earthquake mapped by radar interferometry. Nature 364:138–142

56. Massonnet D, Briole P, Arnaud A (1995) Deflation of Mount Etna monitored by spaceborne radar interferometry. Nature 375:567–570

57. Thatcher W, Massonnet D (1997) Crustal deformation at Long Valley Caldera, eastern California, 1992–1996 inferred from satellite radarinterferometry. Geophys Res Lett 24:2519–2522

58. Wicks C Jr, Thatcher W, Dzurisin D (1998) Migration of fluids Beneath Yellowstone Caldera inferred from satellite radar interferometry. Science 282:458–462

59. Sigmundsson F, Durand P, Massonnet D (1999) Opening of an eruptive fissure and seaward displacement at Piton de la Fournaise volcano measured by RADARSAT satellite radar interferometry. Geophys Res Lett 26:533–536

60. Lu Z, Fatland R, Wyss M, Li S, Eichelberer J, Dean K, Freymueller J (1997) Deformation of New Trident volcano measured by ERS-1 SAR interferometry, Katmai National Park, Alaska. Geophys Res Lett 24:695–698

61. Lu Z, Mann D, Freymueller JT, Meyer DJ (2000) Synthetic aperture radar interferometry of Okmok volcano, Alaska: radar observations. J Geophys Res Solid Earth 105:10791–10806

62. Lu Z, Wicks C, Dzurisin D, Thatcher W, Freymueller JT, McNutt SR, Mann D (2000) Aseismic inflation of Westdahl volcano Alaska, revealed by satellite radar interferometry. Geophys Res Lett 27:1567–1570

63. Lu Z, Wicks C, Power JA, Dzurisin D (2000) Ground deformation associated with the March 1996 earthquake swarm at Akutan volcano Alaska, revealed by satellite radar interferometry. J Geophys Res 105:21483–21495

64. Lu Z, Power JA, McConnell VS, Wicks C, Dzurisin D (2002) Preeruptive inflation and surface interferometric coherence characteristics revealed by satellite radar interferometry at Makushin volcano, Alaska: 1993–2000. J Geophys Res 107:B11

65. Lu Z, Masterlark T, Power J, Dzurisin D, Wicks C (2002) Subsidence at Kiska volcano, Western Aleutians, detected by satellite radar interferometry. Geophys Res Lett 29:18

66. Jonsson S, Zebker K, Cervelli P, Segall P, Garbeil H, Mouginis-Mark P, Rowland S (1999) A shallow-dipping dike fed the 1995 flank eruption at Fernandina volcano, Galapagos, observed by satellite radar interferometry. Geophys Res Lett 26:1077–1080
67. Amelung F, Oppenheimer C, Segall P, Zebker H (2000) Ground deformation near Gada 'Ale volcano, Afar, observed by radar interferometry. Geophys Res Lett 27:3093–3096
68. Pritchard ME, Simons M (2002) A satellite geodetic survey of large-scale deformation of volcanic centres in the central Andes. Nature 418:167–171
69. Goldstein RM, Zebker HA, Werner CL (1988) Satellite radar interferometry – two-dimensional phase unwrapping. Radio Sci 23:713–720
70. Gens R (2003) Two-dimensional phase unwrapping for radar interferometry: developments and new challenges. Int J Remote Sens 24:703–710
71. Sturkell E, Einarsson P, Sigmundsson F, Geirsson H, Olafsson H, Pedersen R, de Zeeuw-van Dalfsen E, Linde AT, Sacks SI, Stefansson R (2006) Volcano geodesy and magma dynamics in Iceland. J Volcanol Geotherm Res 150:14–34
72. Rymer H (1996) Microgravity monitoring. In: Scarpa R, Tilling R (eds) Monitoring and mitigation of volcano hazards. Springer, Berlin
73. Battaglia M, Hill D (2009) Analytical modeling of gravity changes and crustal deformation at volcanoes: the Long Valley Caldera (CA) case study. Tectonophysics 471:45–57
74. Williams-Jones G, Rymer H, Mauri G, Gottsmann J, Poland M, Carbone D (2008) Toward continuous 4D microgravity monitoring of volcanoes. Geophysics 73:WA19–WA28
75. Carbone D, Budettaa G, Greco F, Rymer H (2003) Combined discrete and continuous gravity observations at Mount Etna. J Volcanol Geotherm Res 123:123–135
76. Symonds RB, Gerlach TM, Reed MH (2001) Magmatic gas scrubbing: implications for volcano monitoring. J Volcanol Geotherm Res 108:303–341
77. Doukas MP, Gerlach TM (1995) Sulfur dioxide scrubbing during the 1992 eruption of Crater Peak, Mount Spurr, Alaska. In: Keith T (ed) The 1992 eruptions of Crater Peak Vent, Mount Spurr Volcano, Alaska, U.S. Geological Survey Bulletin B-2139. U.S. G.P.O.: U.S. Dept. of the Interior, US Geological Survey, Washington, DC, pp 47–57
78. Aiuppa A, Moretti R, Federico C, Giudice G, Gurrieri S, Liuzzo M, Papale P, Shinohara H, Valenza M (2007) Forecasting Etna eruptions by real-time observation of volcanic gas composition. Geology 35:1115–1118
79. Werner C, Kelly PJ, Doukas M, Lopez T, Pfeffer M, McGimsey RG, Neal CA (in press) Degassing associated with the 2009 eruption of Redoubt volcano, Alaska. J Volcanol Geotherm Res (Special Issue on the 2009 Redoubt Eruption)
80. Francis P, Horrocks L, Oppenheimer C (2000) Monitoring gases from andesite volcanoes. Philos Trans Math Phys Eng Sci 358:1567–1584
81. Edmonds M (2008) New geochemical insights into volcanic degassing. Philos Trans Math Phys Eng Sci 366:4559–4579
82. Moran SC, Freymueller JT, LaHusen RG, McGee KA, Poland MP, Power JA, Schmidt DA, Schneider DJ, Stephens G, Werner CA, White RA (2008) Instrumentation recommendations for volcano monitoring at US volcanoes under the National Volcano Early Warning System. USGS Scientific Investigations Report 2008–5114
83. Dean KG, Dehn J, Engle K, Izbekov P, Papp K (2002) Operational satellite monitoring of volcanoes at the Alaska Volcano Observatory. In: Harris AJH, Wooster M, Rothery DA (eds) Monitoring volcanic hotspots using thermal remote sensing. Adv Environ Monit Model 1:70–97
84. Mouginis-Mark PJ, Crisp JA, Fink JH (eds) (2000) Remote sensing of active volcanism, AGU Geophysical Monograph 116. American Geophysical Union, Washington, DC
85. Prata J (1989) Observations of volcanic ash clouds in the 10–12 μm window using AVHRR/2 data. Int J Remote Sens 10:751–761
86. Corradini S, Merucci L, Prata AJ, Piscini A (2010) Volcanic ash and SO_2 in the 2008 Kasatochi eruption: retrievals comparison from different IR satellite sensors. J Geophs Res 115:D00L21. doi:10.1029/2009JD013634

87. Schneider DJ, Dean KG, Dehn J, Miller TP, Kirianov VY (2000) Monitoring and analysis of volcanic activity using remote sensing data at the Alaska Volcano Observatory: case study for Kamchatka, Russia, December 1997. In: Mouginis-Mark PJ, Crisp JA, Fink JH (eds) Remote sensing of active volcanism, AGU Geophysical Monograph 116. American Geophysical Union, Washington, DC

88. Zehner E (2010) Monitoring volcanic ash from space. European Space Agency, Noordwijk, p 110

89. Schneider DJ, Vallance JW, Wessels RL, Logan M, Ramsey MS (2008) Use of thermal infrared imaging for monitoring renewed dome growth at Mount St. Helens, 2004. In: Sherrod DR, Scott WE, Stauffer PH (eds) A volcano rekindled; the renewed eruption of Mount St. Helens, 2004–2006, U.S. Geological Survey Professional Paper 1750. U.S. Dept. of the Interior, U.S. Geological Survey, Reston, p 856 and DVD-ROM [http://pubs.usgs.gov/pp/1750/]

90. Wessels RL, Coombs ML, Schneider DJ, Dehn J, Ramsey MS (2010) High-resolution satellite and airborne thermal infrared imaging of the 2006 eruption of Augustine volcano. In: Power JA, Coombs ML, Freymueller JT (eds) The 2006 eruption of Augustine volcano, Alaska, U.S. Geological Survey Professional Paper 1769. U.S. Geological Survey, Reston, pp 527–552

91. Patrick MR, Harris AJL, Ripepe M, Dehn J, Rothery DA, Calvari S (2007) Strombolian explosive styles and source conditions: insights from thermal (FLIR) video. Bull Volcanol 69:769–784

92. Krueger AJ, Schaefer SJ, Krotkov N, Bluth G, Barker S (2000) Ultraviolet remote sensing of volcanic emissions. In: Mouginis-Mark PJ, Crisp JA, Fink JH (eds) Remote sensing of active volcanism, AGU Geophysical Monograph 116. American Geophysical Union, Washington, DC

93. Carn SA, Krueger AJ, Krotkov NA, Yang K, Evans K (2009) Tracking volcanic sulfur dioxide clouds for aviation hazard mitigation. Nat Hazard 51:325–343

94. McNutt SR, Williams ER (2010) Volcanic lightening: global observations and constraints on source mechanisms. Bull Volcanol 72:1153–1167

95. Schilling SP, Thompson RA, Messerich JA, Iwatsubo EY (2008) Use of digital aerophoto-grammerty to determine rates of lava dome growth, Mount St. Helens, Washington, 2004–2005. In: Sherrod DR, Scott WE, Stauffer PH (eds) A volcano rekindled; the renewed eruption of Mount St. Helens, 2004–2006, U.S. Geological Survey Professional Paper 1750. U.S. Dept. of the Interior, U.S. Geological Survey, Reston, p 856 and DVD-ROM [http://pubs.usgs.gov/pp/1750/]

96. Garces MA, Iguchi M, Ishihara K, Morrissey M, Sudo Y, Tsutsui T (1999) Infrasonic precursors to a Vulcanian eruption at Sakurajima volcano, Japan. Geophys Res Lett 26:2537–2540

97. Johnson JB (2003) Generation and propagation of infrasonic airwaves from volcanic explosions. J Volcanol Geotherm Res 121:1–14

98. Johnson JB, Aster RC, Ruiz MC, Malone SD, McChesney PJ, Lees JM, Kyle PR (2003) Interpretation and utility of infrasonic records from erupting volcanoes. J Volcanol Geotherm Res 121:15–63

99. Matoza RS, Fee D, Garces MA, Seiner JM, Ramon PA, Hedlin MAH (2009) Infrasonic jet noise from volcanic eruptions. Geophys Res Lett 36. doi:1029/2008GL036486

100. Caplan-Auerbach J, Bellesiles A, Fernandes JK (2010) Estimates of eruption velocity and plume height from infrasonic recordings of the 2006 eruption of Augustine volcano, Alaska. J Volcanol Geotherm Res 189:12–18

101. Blong R (1996) Volcanic hazards risk assessment. In: Scarpa R, Tilling R (eds) Monitoring and mitigation of volcano hazards. Springer, Berlin

102. Annen C, Wagner J-J (2003) The impact of volcanic eruptions during the 1990s. Nat Hazard Rev 4:169–175

103. Hoblitt RP, Miller CD, Scott WE (1987) Volcanic hazards with regard to siting nuclear-power plants in the Pacific Northwest. U.S. Geological Survey Open-File Report 87-297

104. Siebert L (1996) Hazards of large debris avalanches. In: Scarpa R, Tilling R (eds) Monitoring and mitigation of volcano hazards. Springer, Berlin

105. Ewert JW, Murray T, Lockhart A, Miller C (1993) Preventing volcanic catastrophe: the U. S. International Volcano Disaster Assistance Program. Earthq Volcanoes 24:270–291

106. Wright TL, Pierson TC (1992) Living with volcanoes: The U. S. Geological Survey's Volcano Hazards Program, USGS Circular 1973. United States Government Printing Office, Washington, DC

107. Alvarado GE, Soto GJ, Schmincke H-U, Blge LL, Sumita M (2006) The 1968 andesitic lateral blast eruption at Arenal volcano, Costa Rica. J Volcanol Geotherm Res 157:9–33

108. Fisher RV, Heiken G, Hulen J (1998) Volcanoes: crucibles of change. Princeton University Press, Princeton

109. Holloway M (2000) The killing lakes. Sci Am 283:92–99

110. Sutton AJ, Elias T (1993) Volcanic gases create air pollution on the Island of Hawai'i: U.S. Geological Survey. Earthq Volcanoes 24:178–196

111. Gardner CA, Guffanti MC (2006) U.S. Geological Survey's alert notification system for volcanic activity. U.S. Geological Survey Fact Sheet 2006-3139p

112. Swanson DA, Casadevall TJ, Dzurisin D, Holcomb RT, Newhall CG, Malone SD, Weaver CS (1985) Forecasts and predictions of eruptive activity at Mount St. Helens, USA: 1974–1984. Science 3:397–423

113. Power JA, Jolly A, Nye C, Harbin M (2002) A conceptual model of the Mount Spurr magmatic system from seismic and geochemical observations of the 1992 Crater Peak eruption sequence. Bull Volcanol 64:206–218

114. Ruppert NA, Prejean S, Hansen RA (2011) Seismic swarm associated with the 2008 eruption of Kasatochi volcano, Alaska: earthquake locations and source parameters. J Geophys Res 116:B00B07. doi:10.1029/2010JB007435

115. Abe K (1992) Seismicity of the caldera-making eruption of Mount Katmai, Alaska in 1912. Bull Seismol Soc Am 82:175–191

116. Japan Meteorological Agency (JMA) (2000) Recent seismic activity in the Miyakejima and Niijima-Kozushima region, Japan – the largest earthquake swarm ever recorded. Earth Planets Space 52:i–iv

117. Guffanti M, Diefenbach AK, Ewert JW, Ramsey DW, Cervelli PF, Schilling SP (2008) Volcano-monitoring instrumentation in the United States, 2008. USGS Open-File Report 2009-1165

118. Dzurisin D (2003) A comprehensive approach to monitoring volcano deformation as a window on the eruption cycle. Rev Geophys 41:1–29

119. Benoit JP, McNutt SR (1996) Global volcanic earthquake swarm database and preliminary analysis of volcanic earthquake swarm duration. Annali de Geofisca 39:221–229

120. Power JA, Coombs ML, Freymueller JT (eds) (2010) The 2006 eruption of Augustine volcano, Alaska, U.S. Geological Survey Professional Paper 1769. U.S. Geological Survey, Reston

121. Power JA, Lalla DJ (2010) Seismic observations of Augustine volcano, 1970–2007. In: Power JA, Coombs ML, Freymueller JT (eds) The 2006 eruption of Augustine volcano, Alaska, U.S. Geological Survey Professional Paper 1769. U.S. Geological Survey, Reston, pp 527–552

122. McGee KA, Doukas MP, McGimsey RG, Neal CA, Wessels RL (2010) Emission of SO_2, CO_2, and H_2S from Augustine volcano, 2002–2008. In: Power JA, Coombs ML, Freymueller JT (eds) The 2006 eruption of Augustine volcano, Alaska, U.S. Geological Survey Professional Paper 1769. U.S. Geological Survey, Reston, pp 609–630

123. Neal CA, Murray TL, Power JA, Adleman JN, Whitmore PM, Osiensky JM (2010) Hazard information management, interagency coordination, and impacts of the 2005–2006 eruption of Augustine volcano. In: Power JA, Coombs ML, Freymueller JT (eds) The 2006 eruption of Augustine volcano, Alaska, U.S. Geological Survey Professional Paper 1769. U.S. Geological Survey, Reston, pp 645–667

124. Freymueller JT, Kaufman AM (2010) Changes in the magma system during the 2008 eruption of Okmok volcano, Alaska, based on GPS measurements. J Geophys Res 115: B12415, 14 pp. doi:10.1029/2010JB007716

125. Lu Z, Dzurisin D, Biggs Wicks JC Jr, McNutt S (2010) Ground surface deformation patterns, magma supply, and magma storage at Okmok volcano, Alaska, from InSAR analysis: 1. Intereruption deformation, 1997–2008. J Geophys Res 115:B00B02. doi:10.1029/2009JB006969

126. Larsen J, Neal C, Webley P, Freymueller J, Haney M, McNutt S, Schneider D, Prejean S, Schaefer J, Wessels R (2009) Eruption of Alaska volcano breaks historic pattern. Eos Trans Am Geophys Union 90:173–174

127. Johnson JH, Prejean S, Savage MK, Townend J (2010) Anisotropy, repeating earthquakes, and seismicity associated with the 2008 eruption of Omok volcano, Alaska. J Geophs Res 115. doi:10;1029/2009JB006991

128. Linde AT, Sacks IS (1998) Triggering of volcanic eruptions. Nature 395:888–890

129. Manga M, Brodsky EE (2006) Seismic triggering of eruptions in the far field: volcanoes and geysers. Annu Rev Earth Planet Sci 34:263–291

130. Walter TR, Amelung F (2007) Volcanic eruptions following M > = 9 megathrust earthquakes: implications of the Sumatra-Andaman volcanoes. Geology 35:539–542

131. Hill DP, Pollitz F, Newhall C (2002) Earthquake-volcano interactions. Phys Today 55:41–47

132. Hill DP, Reasenberg PA, Michael AJ, Arabasz WJ, Beroza GC (1993) Seismicity remotely triggered by the magnitude 7.3 Landers, California earthquake. Science 260:1617–1623

133. Prejean SG, Hill DP (2009) Earthquakes, dynamic triggering of. In: Encyclopedia of complexity and system science, editor in-cheif Meyers RA. Complexity in earthquakes, tsunamis, and volcanoes, and forecast, Lee WHK (ed). Springer, Berlin

134. Spudich P, Steck LK, Hellweg M, Fletcher JB, Baker LM (1992) Transient stresses at Parkfield, California, produced by the M 7.4 Landers earthquake of June 28, 1992: observations from the UPSAR dense seismograph array. J Geophys Res 100:675–690. doi:10.1029/94JB02477

135. McGee KA, Doukas MP, Kessler R, Gerlach TM (1997) Impacts of volcanic gases on climate, the environment, and people. U.S. Geological Survey Open-File 97-262

136. Robb LJ (2005) Introduction to ore-forming processes. Blackwell Science, Carlton

137. Peterson DW (1996) Mitigation measures and preparedness plans for volcanic emergencies. In: Scarpa R, Tilling R (eds) Monitoring and mitigation of volcano hazards. Springer, Berlin

138. Self S (2006) The effects and consequences of very large explosive volcanic eruptions. Philos Trans R Soc A 364:2073–2097

139. Simkin T, Siebert L, Blong R (2001) Volcano fatalities: lessons from the historical record. Science 291:255

140. Ewert JW, Harpel CJ (2004) In harm's way: population and volcanic risk. Geotimes 49:14–17

141. International Air Travel Association (2010) Volcano crisis cost airlines $1.7 billion in revenue – IATA urges measures to mitigate impact, IATA press release

142. USGS (1997) Volcanic ash – danger to aircraft in the North Pacific. U.S. Geological Survey Fact Sheet 030-97

143. Geothermal Energy Association (2010) Geothermal energy: international market update, 7 pp

144. U.S. Energy Information Administration (2009) Annual Energy Review

145. Ewert JW, Guffanti M, Murray TL (2005) An assessment of volcanic threat and monitoring capabilities in the United States: framework for a National Volcano Early Warning System. USGS Open-File Report 2005-1164

146. Song W-Z, Shirazi B, Huang BR, Xu M, Peterson N, LaHusen R, Pallister J, Dzurisin D, Moran S, Lisowski M, Kedar S, Chien S, Webb F, Kiely A, Doubleday J, Davies A, Pieri D (2010) Optimized autonomous space in-situ sensor web for volcano monitoring. IEEE J Sel Topics Appl Earth Observ Remote Sens 3:541–546

147. Fleming K, Picozzi M, Milkereit C, Kuehnlenz F, Lichtblau B, Fischer J, Zulfikar C, Oezel O, Zschau J, Veit I, Jaeckel KH, Hoenig M, Nachtigall J, Woith H, Redlich JP, Ahrens K,

Eveslage I, Heglmeier S, Erdik M, Kafadar N (2009) The self-organizing seismic early warning information network (SOSEWIN). Seismol Res Lett 80:755–771

148. Huang R, Song W-Z, Xu M, Picone N, Shirazi B, LaHusen R (2011) Real-world sensor network for long-term volcano monitoring: design and findings. IEEE Trans Parallel Distrib Syst 99, doi:10.1109/TPDS.2011.170